

Self-directed Joint Research of MERIT program

Investigation of shrinking mechanism of fused porphyrin-based porous crystal via x-ray diffraction under variable temperature-pressure conditions

¹Shun Suginome, ²Keishiro Yamashita

¹ Department of Chemistry and Biotechnology, School of Engineering, The University of Tokyo

² Geochemical Research Center, Graduate School of Science, The University of Tokyo

Author Contributions

S. Suginome: Specialise in supramolecular chemistry and materials chemistry. In this study, he synthesised the sample, evaluated them and measured x-ray diffraction at low/high temperatures.

K. Yamashita: Specialise in high-pressure physical chemistry. He measured x-ray diffraction under high pressure.

Abstract

Although "soft" metal-organic frameworks (MOFs) attract much attention recently, there are still few comprehensive studies that correlate the structural changes of a MOF induced by different types of external stimuli. In this study, to understand the mechanism of the contraction phenomenon of a MOF based on fused porphyrin (^{Fused}MOF) discovered by the author, the structural changes of ^{Fused}MOF under both high temperature (< 420 K) and high pressure (< 2.2 GPa) conditions were investigated by variable temperature powder X-ray diffraction measurements at Spring-8 and by variable pressure powder X-ray diffraction measurements using a DAC. In the region of 250-360 K at atmospheric pressure or below 0.5 GPa at room temperature, ^{Fused}MOF showed a continuous decrease in unit-cell volume by 1.7% on heating and 2.4% on pressurisation. These volume changes are much larger than those observed for other well-known MOFs such as MOF-5, which characterizes ^{Fused}MOF with extremely large pore volumes. Face-centred cubic lattice was maintained under high-temperature conditions, while the symmetry of the lattice decreased under high-pressure conditions > 0.5 GPa.

1 Background and objectives

Porous materials such as activated carbons and zeolites have been investigated from the expectation of their application towards molecular sieve, gas adsorption, and reaction field of adsorbed chemical species. In recent years, the metal-organic framework (MOF) gathers scientific and industrial attention as a new candidate for a porous crystalline material.¹ MOF is characterised by its framework structure composed of organic ligands and coordinated metal ions. MOF can be designed to have demanded pores homogeneously because of the enormous combinations of the ligands and the metal ions as building units. This advantage on the designability enhanced scientists to develop various kinds of

MOFs in different scopes such as gas adsorption and separation, catalyst, drug delivery, *etc.* MOF is known as a “soft” material that changes its crystal structure by external stimulations such as heat, light, electric field, and pressure. This flexible property is in contrast to rigid materials like most other porous materials.² However, there are limited numbers of comprehensive studies on the structural variations of MOF based on different external stimulations.

The structural changes in MOF do not come only from MOF itself but also depends on the guest molecules incorporated into the MOF pores. Molecules confined in the pores of the nano-metre scale are strongly affected by the interface between the MOF so that they show anomalous behaviours compared with their bulk state. For instance, water molecules form pseudo-one-dimensional clusters in carbon nanotubes³ or hydrophilic molecular crystals with pseudo-one-dimensional nano-channel.⁴ Again, MOF is a “soft” material, so that such anomalous behaviours of the incorporated guest molecules affect the framework of MOF. Therefore, it needs comprehensive investigation from various perspectives using different parameters like temperatures and pressure to understand the physical and chemical properties of MOF.

We found that a newly synthesized MOF based on fused porphyrin⁵ (^{Fused}MOF, Fig. 1) shows intriguing structural changes.⁶ By irradiation of near-infrared light to ^{Fused}MOF immersed in DMF, the crystal contracted rapidly and reversibly as if they were compressed from the outside (Fig. 2). The structural change may be due to the following mechanisms: 1. ^{Fused}MOFs have an absorption band in the near-infrared region associated with electronic transitions; 2. local heat is generated in the vicinity of the ligand (photothermal effect) when the fused porphyrin moieties are excited through near-infrared irradiation and decayed in a non-radiative manner; 3. ^{Fused}MOF has a huge void space that encapsulates 2,000 *N,N*-dimethylformamide (DMF) molecules per unit cell. The heat generated in the vicinity of the ligand causes partial desorption of the solvent molecules, resulting in a structural distortion.

In this study, we first examined the shrinking mechanism hypothesised above from the temperature dependence of the structure of the ^{Fused}MOF from x-ray diffraction. Moreover, ^{Fused}MOF has quite

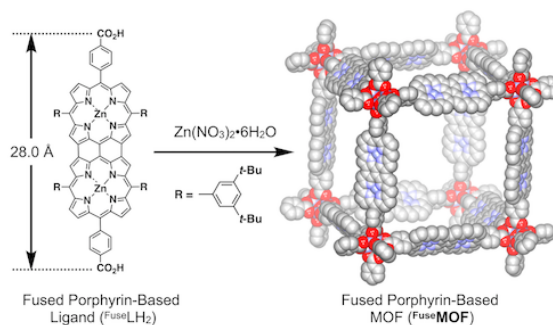


Figure 1: Synthesis and crystal structure of ^{Fused}MOF. 3,5-di-*tert*-butylphenyl groups are not displayed for clarity.

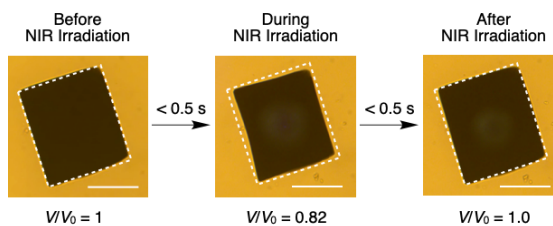


Figure 2: Reversible contraction-expansion of ^{Fused}MOF upon NIR light irradiation (Scale Bar: 100 μm).

large pores with a diameter of 4.0 nm and is expected to have structural flexibility. Thus we also examined the pressure dependence of its crystal structure. This study aims to provide new findings of the structural changes of MOF related to entry and exit of guest molecules under external stimulation, temperature and pressure.

2 Experimental

In-situ x-ray diffraction experiments were conducted at high/low temperatures or high pressures to reveal the structural changes of ^{Fused}MOF induced by temperature or pressure.

1) Synthesis of ^{Fused}MOF and MOF-5

Fused porphyrin-based dicarboxylic acid ligand ^{Fused}LH₂ (Fig. 1, left) was synthesized in two steps (60% overall yield) starting from porphyrin monocarboxylic acid methyl ester.⁷ ^{Fused}MOF was obtained as purple cube-shaped crystals in 23% yield by the reaction of ^{Fused}LH₂ and zinc nitrate hexahydrate in *N,N*-diethylformamide (DEF) at 120 °C for 20 h. As-synthesized ^{Fused}MOF was washed once with DEF and then three times with DMF prior to the measurements. MOF-5 was synthesized according to the literature by Yaghi *et al.*⁸

2) X-ray diffraction experiments

2-1) Heated/cooled condition under ambient pressure

X-ray diffraction experiments at high/low temperatures were conducted at the BL02B2 beamline of the Spring-8 ($\lambda = 0.8000 \text{ \AA}$). Powder ^{Fused}MOF was sealed into a capillary with DMF. Diffraction patterns were collected in temperature ranges from 210 to 420 K in which the DMF is in liquid phase at ambient pressure. Details of the measurement scheme are the following.

a) Low-temperature region: the specimen was first cooled down to 210 K and heated step by step with intervals of 10 K up to 300 K. Diffraction patterns were collected at each step.

b) High-temperature region: diffraction patterns at temperatures 300 K up to 420 K with intervals of 10 K were collected using the specimen after the measurement a). Before heating up to the next (higher) temperature, the sample was cooled down to 300 K and a diffraction pattern was collected at 300 K to examine the reversible changes. In more detail, the diffraction patterns were collected in the following order: 300 K, 310 K, 300 K, 320 K, ... 410 K, 300 K, 420 K, 300 K.

The unit-cell volume, V , at each temperature was derived by peak fitting analysis of the obtained diffraction profile using *Conograph*⁹ software.

2-2) High-pressure condition under ambient temperature

X-ray diffraction experiments at high pressures from atmospheric pressure to 2.2 GPa were conducted at our laboratory using a micro-focused x-ray source (Rigaku, MicroMax-007, MoK α) and

an imaging-plate detector (Rigaku MicroMax-007). Powder FusedMOF and DMF were used as starting materials as done in the temperature-controlled experiment. The sample compression was done by diamond anvil cells equipping Bohler-Almax type¹⁰ diamond anvils with a culet diameter of $\phi = 800 \mu\text{m}$ (Figure 3). A Stainless 301 plate of thickness $t = 0.2 \text{ mm}$ was used as a gasket after drilling with the diameter of $\phi = 0.4 \text{ mm}$ for the sample space. Almost identical high-pressure experiments were also conducted for MOF-5⁸ for comparison. MOF-5 is a representative MOF with a cubic structure similar to FusedMOF .

The obtained two-dimensional diffraction patterns were reduced into one-dimensional profiles using *IPAnalyzer*¹¹. The tilt or distortion of the detector was corrected in the conversion procedures based on calibration using silver behenate ($[\text{Ag}(\text{O}_2\text{C}_{22}\text{H}_{43})]_2$; $a = 4.1769 (2) \text{ \AA}$, $b = 4.7218 (2) \text{ \AA}$, $c = 58.3385 (1) \text{ \AA}$, $\alpha = 89.440 (3)^\circ$, $\beta = 89.634 (3)^\circ$, $\gamma = 75.854 (1)^\circ$ ¹²) who has numbers of diffraction peaks at high- d region. The unit-cell volume, V , at each pressure was derived by peak fitting analysis of the obtained diffraction profile using *PDIndexer*¹¹ software.

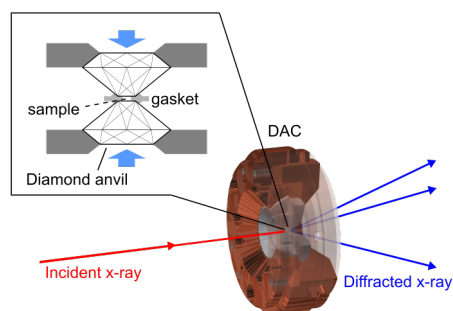


Figure 3: Schematic image of diamond anvil cell (DAC) and diffraction geometry in the high-pressure experiment. Inset shows close-up view around the sample space.

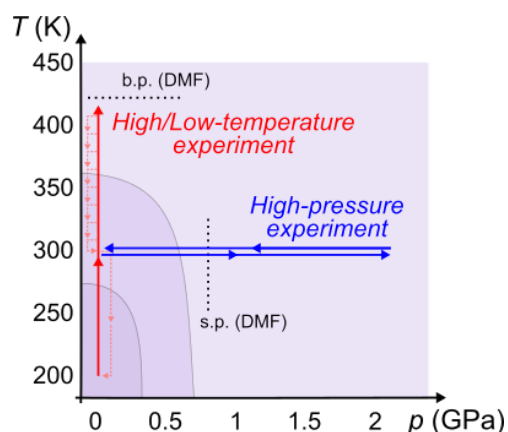


Figure 4: Illustration of temperature-pressure regions in this study. Each coloured region corresponds to the area in which the behaviours of FusedMOF would be different. The boiling point (b.p.: 426 K) at atmospheric pressure and melting point (s.p.: 0.78 GPa) at ambient temperature of the coexisting solvent, DMF, are described by dot lines.

3 Results and discussions

The temperature dependence of the crystal structure of FusedMOF was examined in 210–420 K. The obtained diffraction profiles did not change drastically nor diminish (Figure 5), which means the crystallinity of the sample was retained during the experiment. The representative peaks (200, 200, 220, 400, 440, 600, 620 reflections) remain observable and no new peak emerged. These indicate that the heated FusedMOF retains its face-centred cubic structure. All diffraction peaks shift towards higher 2θ . The derived unit-cell volumes V monotonically decreased according to the temperature elevation

(Figure 6). This phenomenon is called negative thermal expansion and getting to be a target of material science. The structure of $^{\text{Fused}}\text{MOF}$ shrank by 1.7% at 420 K from at 210 K. $^{\text{Fused}}\text{MOF}$ shrank at a higher rate than the existing materials.¹³ Note that this experiment was conducted under the condition of coexistence of solvent. It characterises our study in the situation of entry and exit of the guest molecules into and from the MOF pores. In other words, our findings imply that MOF structure shrinks by desorption of the guest molecules from the pores and this effect overwhelms the typical expansion by large thermal motions at high temperatures. The diffraction profile at 300 K after recovery from 420 K was identical to the profile obtained at the beginning of this experiment. The observed shrinkage of $^{\text{Fused}}\text{MOF}$ induced by temperature changes is considered to be reversible.

Here, the observed negative thermal expansion can be classified into three

types by temperature regions in 200–250, 250–360, 360–420 K expecting the behaviours of DMF. Assuming linear relation, the thermal expansion coefficients in the regions were -5.49×10^{-5} , -1.08×10^{-4} , $-4.92 \times 10^{-5} \text{ K}^{-1}$, respectively, and the middle-temperature region had the steepest slope. These differences in the shrinkage trends imply that the interactions among DMF and between MOF and DMF vary by the temperature regions. This would be induced by the difference in the packing scheme of DMF molecules in the MOF pores. These behaviours highlight the characteristic of $^{\text{Fused}}\text{MOF}$ and are qualitatively consistent with the shrinkage under irradiation by near-infrared light. Nevertheless, the macroscopic volume decrease observed under irradiation was quite larger than this high-temperature experiment. The irradiated case would contain other factors than the heating such as

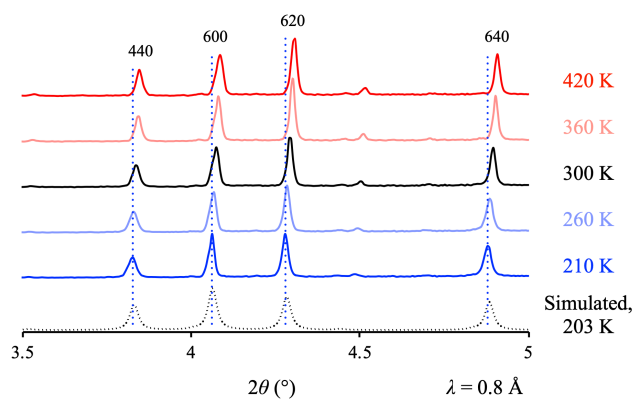


Figure 5: Diffraction profiles of $^{\text{Fused}}\text{MOF}$ heated/cooled in DMF (ambient pressure, 210 K–420 K). Peak positions at 210 K are described by blue dot lines. For comparison, a simulated pattern based on a single-crystal x-ray diffraction at 203 K is shown by a dot line.

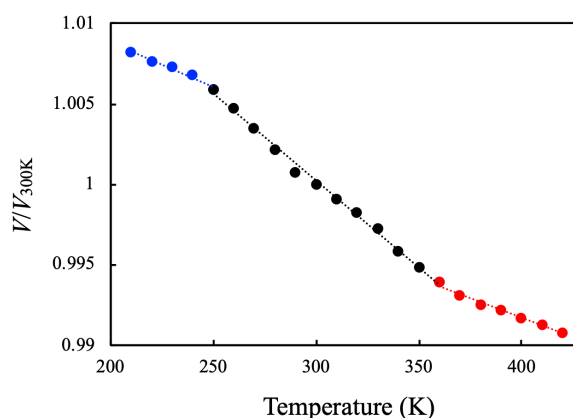


Figure 6: Temperature dependence of unit-cell volume V of $^{\text{Fused}}\text{MOF}$ normalised by the value at 300 K. Linear regression lines for temperature regions of 210–250, 250–360, 360–420 K are displayed by dot lines.

activation by light, temperature difference inside/outside of the crystal, and diffusion of DMF molecules.

Next, the structural changes of FusedMOF and its reversibility against compression were examined by high-pressure x-ray diffraction up to 2.2 GPa. Figure 7 shows the representative profiles. During compression up to 0.4 GPa, the diffraction peaks monotonically shifted to higher 2θ indicating volume decrease without drastic profile changes. The unit-cell volume decreased by 2.4% at 0.4 GPa from the value before compression. The bulk modulus of FusedMOF was estimated to be $\kappa = 11$ GPa by linear regression (Figure 8, red lines). This value is

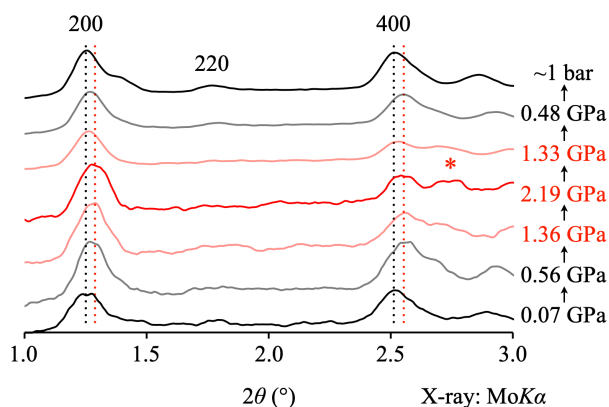


Figure 7: Pressure dependent diffraction profiles of FusedMOF at ambient temperature. Peak positions of 200 and 400 are described by black dot lines (ambient pressure) and red dot lines (high pressure). A new peak observed at high pressures is indicated by asterisk (*).

smaller than $\kappa = 343$ GPa (Figure 8, black lines) of the MOF-5⁸ derived in this study. The derived bulk modulus of MOF-5 is consistent with the reported value using DEF as coexisting solvent¹⁴. MOF-5 is isostructural with FusedMOF . Our observation clarified the distinct structural flexibility of FusedMOF despite its structural similarity to MOF-5. This large volume decrease is considered to be related to detachments of DMF molecules like the case of the negative thermal expansion observed in the high-temperature experiment.

Whereas the crystal structure of FusedMOF was identical to the ambient condition below 0.5 GPa, diffraction profiles changed over the pressure: *e.g.* intensity decrease of a 400 peak and emergence of a new peak at *ca.* $2\theta = 2.7^\circ$. Moreover, 200 and 400 peaks once shifted to higher angle according to compression in 0.6–1 GPa and shift again to lower angle over 1 GPa (Figure 7, 9). Before moving to the decompression experiment, the sample was left overnight for relaxation because the solvent DMF crystallised at 2.2 GPa. The reported solidification pressure of DMF was *ca.* 0.8 GPa¹⁵, but it remains in the liquid phase up to 2.2 GPa during the compression. Regarding the mismatch between d_{400} during compression and decompression (Figure 9), the sample space seemed to lose the hydrostaticity over 1 GPa. On the other hand, the pressure dependences below 1 GPa were reproduced in decompression such as a minimum of d_{400} at 0.6 GPa. After sample recovery to ambient pressure, the peak profiles and unit-cell volumes got back into the original ones (Figure 7). It is not clear the hydrostaticity in compressed DMF and its effect on the compression behaviour of FusedMOF , but the observation that the non-monotonic shift of certain diffraction peaks such as 400 and the change of the peak profile

indicates the symmetry change from original cubic over 0.5 GPa. Based on the fact that the structural changes of $^{\text{Fused}}\text{MOF}$ during compression and decompression was reversible, drastic change such as bond-dissociation and reconstruction of the framework is less plausible. Thus, the high-pressure structure of the $^{\text{Fused}}\text{MOF}$ is expected to be rhombohedral by distortion retaining the bonding topology. This hypothesis provides an expectation of the structural control of $^{\text{Fused}}\text{MOF}$ retaining the designed bonding and coordinating structure.

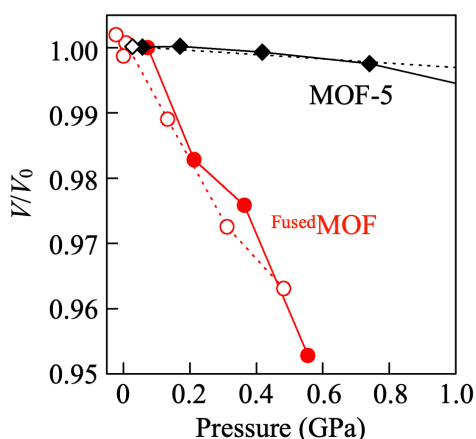


Figure 8: Pressure dependences of unit-cell volumes of $^{\text{Fused}}\text{MOF}$ (red) and MOF-5 (black). The values are normalised by that before compression. Solid and dot lines indicates the compression and decompression procedures, respectively. The plots of $^{\text{Fused}}\text{MOF}$ is extracted in the region in which the original cubic structure is expected to remain.

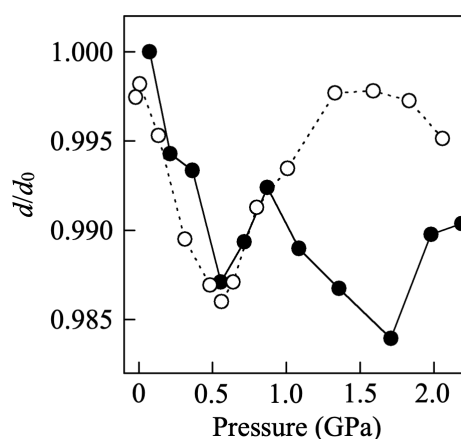


Figure 9: Pressure dependence of d_{400} of $^{\text{Fused}}\text{MOF}$. Solid and dot lines indicates the compression and decompression procedures, respectively. The values are normalised by that before compression.

Our observation indicates that $^{\text{Fused}}\text{MOF}$ can retain its original crystal structure at the ambient condition up to 0.5 GPa at room temperature and in 250–360 K at ambient pressure. Thus the DMF in the framework is expected to behave similarly (Figure 4). On the other hand, $^{\text{Fused}}\text{MOF}$ showed different behaviours in harsher conditions: the gentle slope of negative thermal expansion over 360 K at ambient pressure and symmetry reduction of the crystal structure over 0.6 GPa at room temperature. Based on the consideration of the behaviours of DMF molecules, these behaviours in harsh conditions are considered to be related to the state after a certain amount of DMF exited from the framework. However, there were obvious differences in the structure symmetry, *i.e.* $^{\text{Fused}}\text{MOF}$ retained its face-centred cubic symmetry at high temperatures but did not at high pressures. These differences would be related to the support by the DMF molecules in the framework. At high temperatures, the framework is supported by the DMF molecules inside which move with energy by thermal motion while the DMF no longer can support the framework at a higher pressure than 0.6 GPa at room temperature. Thus, our result implies that the behaviours of DMF incorporated into the MOF strongly affect the physical properties of MOF itself. *In-situ* single-crystal diffraction study will provide more

direct information on the number of DMF molecules in the framework and their packing structure¹⁴, but this is out of our scope here because of the difficulty of retaining the crystallinity.

4 Conclusion

In this study, the mechanism of structural changes of ^{Fused}MOF was investigated by synchrotron x-ray diffraction under high/low temperature at the Spring-8 and x-ray diffraction under high pressure. ^{Fused}MOF showed reversible changes in 210–420 K at ambient pressure or pressures below 2.2 GPa at room temperature, but some different trends were found in regions divided by temperature and pressure respectively. ^{Fused}MOF showed a monotonic decrease in unit-cell volume in relatively mild conditions in 250–360 K at ambient pressure or below 0.5 GPa at room temperature. The smallest volumes resulted in decreases from the ambient conditions by 1.7% during heating and 2.4% during compression in these regions. On the other hand, the negative thermal expansion coefficient became almost half of that in ambient temperature region in temperature regions of 200–250 and 360–420 K. The compression behaviour of ^{Fused}MOF also differed over 0.5 GPa from the lower pressure region, indicating that the ^{Fused}MOF lose its face-centred cubic symmetry. These findings highlight the characteristics of ^{Fused}MOF which has quite large pores and is strongly affected by circumstances compared to other known MOFs like MOF-5. Such volume changes are caused not only by the structural changes in the framework itself but also by a complicated mechanism related to interactions between DMF and MOF or among DMF molecules. This perspective based on the interaction between the host framework and guest molecules brings about an interest in further studies using different solvents for comparison. Moreover, the qualitative and systematic verification for the detailed behaviours of ^{Fused}MOF can be done by *in-situ* experiments based on the combination of external high-pressure and temperature experiments. Such an experimental approach provides fundamental and directive knowledge to us towards the application of highly-designable MOFs which are prospected to be effective porous material to solve long-standing issues.

Acknowledgements

We gratefully thank Prof. T. Aida and Prof. H. Kagi for their help as our supervisors. We also appreciate the support of Prof. S. Kobayashi and Prof. S. Tsuneyuki, our assistant supervisors. In the end, we would like to express our sincere gratitude to all the staff members of the MERIT programme for providing us with this chance of collaborative work.

References

- (1) Collings, I. E.; Goodwin, A. L. Metal–Organic Frameworks under Pressure. *J. Appl. Phys.* **2019**, *126*, 181101.
- (2) Horike, S.; Shimomura, S.; Kitagawa, S. Soft Porous Crystals. *Nat. Chem.* **2009**, *1*, 695–704.
- (3) Maniwa, Y.; Kataura, H.; Abe, M.; Udaka, A.; Suzuki, S.; Achiba, Y.; Kira, H.; Matsuda, K.;

- Kadowaki, H.; Okabe, Y. Ordered Water inside Carbon Nanotubes: Formation of Pentagonal to Octagonal Ice-Nanotubes. *Chem. Phys. Lett.* **2005**, *401*, 534–538.
- (4) Watanabe, K.; Oguni, M.; Tadokoro, M.; Nakamura, R. Structural Ordering and Ice-like Glass Transition on Cooling the Nano-Channel Water Formed within a Crystalline Framework. *J. Phys. Condens. Matter* **2006**, *18*, 9375–9384.
- (5) Tsuda, A. Fully Conjugated Porphyrin Tapes with Electronic Absorption Bands That Reach into Infrared. *Science* **2001**, *293*, 79–82.
- (6) Suginome, S.; Sato, H.; Araoka, F.; Aida, T. *to be submitted*.
- (7) Imahori, H.; Tamaki, K.; Araki, Y.; Sekiguchi, Y.; Ito, O.; Sakata, Y.; Fukuzumi, S. Stepwise Charge Separation and Charge Recombination in Ferrocene-*meso,meso*-Linked Porphyrin Dimer–Fullerene Triad. *J. Am. Chem. Soc.* **2002**, *124*, 5165–5174.
- (8) Li, H.; Eddaoudi, M.; O’Keeffe, M.; Yaghi, O. M. Design and Synthesis of an Exceptionally Stable and Highly Porous Metal-Organic Framework. *Nature* **1999**, *402*, 276–279.
- (9) Oishi-Tomiyasu, R. Robust Powder Auto-Indexing Using Many Peaks. *J. Appl. Crystallogr.* **2014**, *47*, 593–598.
- (10) Boehler, R.; De Hantsetters, K. New Anvil Designs in Diamond-Cells. *High Press. Res.* **2004**, *24*, 391–396.
- (11) Seto Y.; Nishio-Hamane D.; Nagai T.; Sata N. Development of a Software Suite on X-ray Diffraction Experiments. *Rev. High Press. Sci. Technol.* **2010**, *20*, 269–276.
- (12) Blanton, T. N.; Rajeswaran, M.; Stephens, P. W.; Whitcomb, D. R.; Misture, S. T.; Kaduk, J. A. Crystal Structure Determination of the Silver Carboxylate Dimer $[\text{Ag}(\text{O}_2\text{C}_{22}\text{H}_{43})]_2$, Silver Behenate, Using Powder X-Ray Diffraction Methods. *Powder Diffr.* **2011**, *26*, 313–320.
- (13) Takenaka, K.; Okamoto, Y.; Shinoda, T.; Katayama, N.; Sakai, Y. Colossal Negative Thermal Expansion in Reduced Layered Ruthenate. *Nat. Commun.* **2017**, *8*, 14102.
- (14) Graham, A. J.; Allan, D. R.; Muszkiewicz, A.; Morrison, C. A.; Moggach, S. A. The Effect of High Pressure on MOF-5: Guest-Induced Modification of Pore Size and Content at High Pressure. *Angew. Chem. Int. Ed.* **2011**, *50*, 11138–11141.
- (15) Ratajczyk, P.; Sobczak, S.; Katrusiak, A. High-Pressure Structure and Properties of *N,N*-Dimethylformamide (DMF). *Cryst. Growth Des.* **2019**, *19*, 896–901.